Inorganic Chemistry

Article

pubs.acs.org/IC

Ferroelectric Mesocrystals of Bismuth Sodium Titanate: Formation Mechanism, Nanostructure, and Application to Piezoelectric Materials

Dengwei Hu,[†,‡] Xingang Kong,[§] Kotaro Mori,[†] Yasuhiro Tanaka,[†] Kazunari Shinagawa,[†] and Qi Feng*[,†,⊥]

[†]Department of Advanced Materials Science, Faculty of Engineering, Kagawa University, 2217-20 Hayashi-cho, Takamatsu-shi, 761-0396 Japan

[‡]Department of Chemistry and Chemical Engineering, Baoji University of Arts and Science, 1 Gaoxin Road, Baoji, Shaanxi, 721013 People's Republic of China

[§]School of Materials Science and Engineering, Shaanxi University of Science and Technology, Weiyang, Xi'an, Shaanxi, 710021 People's Republic of China

Supporting Information

ABSTRACT: Ferroelectric mesocrystals of $Bi_{0.5}Na_{0.5}TiO_3$ (BNT) with [100]-crystal-axis orientation were successfully prepared using a topotactic structural transformation process from a layered titanate $H_{1.07}Ti_{1.73}O_4{\cdot}nH_2O$ (HTO). The formation reactions of BNT mesocrystals in HTO−Bi_2O_3−Na_2CO_3 and HTO−TiO_2−Bi_2O_3−Na_2CO_3 reaction systems and their nanostructures were studied by XRD, FE-SEM, TEM, SAED, and EDS, and the reaction mechanisms were given. The BNT mesocrystals are formed by a topotactic structural transformation mechanism in the HTO−Bi_2O_3−Na_2CO_3 reaction system and by a combination mechanism of the topotactic structural transformation and epitaxial crystal growth in the HTO−TiO_2−Bi_2O_3−Na_2CO_3 reaction system, respectively. The BNT mesocrystals prepared by these methods are constructed from [100]-oriented BNT nanocrystals. Furthermore, these reaction systems were successfully applied to the fabrication of [100]-oriented BNT ferroelectric ceramic materials. A BNT ceramic material with a high degree of orientation, high relative density, and small grain size was achieved.

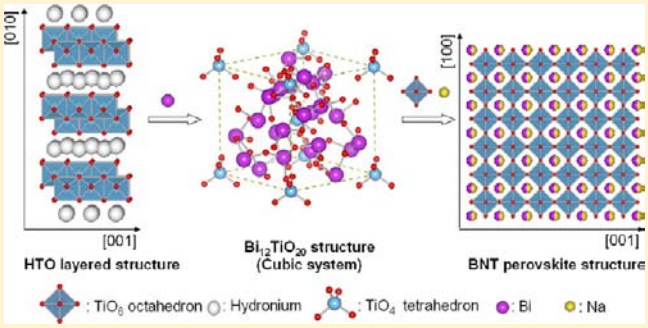

INTRODUCTION

Piezoelectric materials are commonly used in sensor, actuator, and transducer technologies because of their unique ability to couple electrical- and mechanical-energy transformations.[1] In recent years, lead-free piezoelectric materials have attracted considerable attention because of the consideration of environmental protection.[2−4] Bismuth sodium titanate ($Bi_{0.5}Na_{0.5}TiO_3$, BNT) is a well-known ferroelectric material.[5,6] BNT has a perovskite structure with a rhombohedral *R*3*c* space group (a = 38.91 nm; α = 89.6°)[7] at room temperature. In the perovskite structure with the ABO_3 formula, where half of the A site is filled with bismuth(III) and the other half with sodium(I) and the B site is filled with titanium(IV).[8,9] BNT has been considered to be one of the most promising candidate materials for the development of lead-free piezoelectric materials because of its relatively large remnant polarization (P_r = 38 μC/cm^2) and high Curie temperature (T_c = 320 °C).[10,11] Similar to most of the other lead-free piezoelectric materials, the piezoelectricity of BNT is lower than that of lead-based piezoelectric materials,[12−14] so many attempts to improve the physical properties of BNT have been carried out by various methods.

There are two kinds of effective techniques to enhance the piezoelectricity. One is domain engineering for control of the domain size, and the other is texture engineering for control of the orientation direction of the piezoelectric materials. Enhancement of the piezoelectricity and reduction of ferroelectric hysteresis for piezoelectric materials can be realized well by decreasing the domain size,[15,16] and the domain size can be decreased by reducing the grain size of the material.[17] Because ferroelectric materials show crystal-axis anisotropy, their piezoelectricity and permittivity are tensor quantities and relate to both the direction of the applied stress and the electric field.[18] Therefore, high piezoelectricity can be achieved by using crystal-axis-oriented materials as well.[19] It has been reported that the [110]-oriented $BaTiO_3$ ceramic material shows a piezoelectric constant d_{33} value of 788 pC/N,[20] which is much larger than 190 pC/N for the normal $BaTiO_3$ ceramic materials.[21] Consequently, the small grain size and high degree of orientation ceramics with high density are expected for high-performance piezoelectric materials.

Received: June 17, 2013
Published: August 26, 2013

   dx.doi.org/10.1021/ic4015256 | *Inorg. Chem.* 2013, 52, 10542−10551

Templated grain growth (TGG) and reactive-templated grain growth (RTGG) methods have been developed for the fabrication of oriented ceramic materials.[22,23] In these methods, template particles with platelike or fiberlike morphology are necessary because they can be oriented easily via mechanical methods. [100]-,[24,25] [001]-,[26,27] [110]-,[19,20] and [111]-oriented[28,29] perovskite ferroelectric ceramic materials, such as BNT, $BaTiO_3$, BNT−$BaTiO_3$, $Ba_{0.6}Sr_{0.4}TiO_3$, and $Ba_{1-x}Ca_xTiO_3$, have been developed using the TGG or RTGG method. Two kinds of platelike particles, $Bi_4Ti_3O_{12}$[23,30] and $Na_{0.5}Bi_{4.5}Ti_4O_{15}$,[31] have been reported to be used as templates for the fabrication of oriented BNT ceramic materials by the TGG or RTGG method.[23,30,32] These platelike particles were prepared using the solid-state reaction or melt-salt methods, which gives large-size particles.[33−35] Oriented ceramic materials with small grain size and high density are difficult to achieve using these large platelike particles as the templates.[23,30,32]

Up to now, BNT particles have been synthesized using molten-salt,[31,35−38] solid-state,[39] hydrothermal,[40−43] sol−gel,[44,45] vibromilling,[46] and slurry synthesis methods.[47] However, the obtained BNT particles show a cubic or spherical isotropic morphology except when an anisotropic morphology precursor is used. BNT platelike particles have been prepared using the molten-salt method with $Bi_4Ti_3O_{12}$,[35] $Na_{0.5}Bi_{4.5}Ti_4O_{15}$,[31,37] and $Bi_2Ti_4O_{11}$[38] platelike particles as the precursors. The obtained BNT platelike particles have been used as the template to fabricate oriented BNT ceramic materials by the TGG method.[31] However, the high degree of orientation, high density, and small grain size ceramic materials have not been achieved because of the large size and low aspect ratio of BNT platelike templates.

We have reported that a layered titanate $H_{1.07}Ti_{1.73}O_4{\cdot}nH_2O$ (HTO) with a lepidocrocite-like structure and a small platelike particle size of 200 nm thickness and 3 μm width can be prepared by a hydrothermal reaction.[48−50] The HTO platelike particles have been used as precursors for the syntheses of perovskite $BaTiO_3$, $Ba_{1-x}Ca_xTiO_3$, and $Ba_{1-x}(Bi_{0.5}K_{0.5})_xTiO_3$ platelike particles by solvothermal reactions.[19,49−51] The platelike particles of perovskite titanates prepared by this method are constructed from spherical nanoparticles, and all of the spherical nanoparticles of perovskite titanates in the platelike particles align and show the same [110]-direction orientation, forming [110]-oriented platelike particles.[19,49,51] The formation mechanisms of the oriented platelike particles are in situ topotactic transformation reactions, where the metal ions are intercalated into the HTO crystal bulk through an interlayer pathway by an exchange reaction and then react with the layered titanate.

These oriented platelike perovskite polycrystals are a new class of mesocrystals. The mesocrystal is defined as an orientational superstructure with nanometer to micrometer size, which is made from well-aligned oriented crystalline nanoparticles.[52,53] The concept of a mesocrystal has just recently been brought forward and developed in 2003,[53] in order to explain that crystal growth may be a crystalline aggregation-based process via mesoscale transformation. The mesocrystals, which are assemblies of crystallographically oriented nanocrystals, have potential applications to catalysis, sensing, and energy storage and conversion.[52,54,55] We think that the platelike perovskite mesocrystals are a promising material to fabricate the high degree of orientation, high density, and small grain size ceramic materials for high-performance piezoelectric materials. To the best of our knowledge, studies on the syntheses of BNT mesocrystals and other perovskite titanate mesocrystals by the heat-treatment method using HTO as a precursor and also on the fabrication of oriented ceramic materials using the HTO template have not been reported.

In the present study, we describe a new challenge on the synthesis of platelike BNT ferroelectric mesocrystals from the platelike HTO particle precursor using the heat-treatment method, the studies on the formation reaction mechanism and nanostructure, and application of the heat-treatment process to the fabrication of crystal-axis-oriented BNT ceramic materials. The platelike BNT particle prepared via this method is constructed from the aligned nanoparticles, and each nanoparticle shows the same [100] orientation, namely, [100]-oriented BNT mesocrystals. [100]-oriented BNT ceramic materials with a high degree of orientation, high density, and small grain size can be achieved by application of the heat-treatment process to ceramic fabrication using the platelike HTO particles as the template. Success in the fabrication of such BNT ferroelectric ceramic materials is a significant milestone to challenge the high-performance lead-free piezoelectric materials by applying both domain and texture engineering to the piezoelectric ceramics simultaneously.

EXPERIMENTAL SECTION

Materials. All reagents used in this study were of analytical grade and were used without further purification. Bi_2O_3, Na_2CO_3, and TiO_2 (anatase) were purchased from Wako Pure Chemical Industries, Ltd. A platelike $H_{1.07}Ti_{1.73}O_4{\cdot}nH_2O$ (HTO) powder sample was prepared by the acid treatment of $K_{0.8}Ti_{1.73}Li_{0.27}O_4$, which was synthesized by a hydrothermal method reported in the literature.[50]

Synthesis of BNT Powder Samples. Three kinds of titanium sources, namely, platelike HTO particles, anatase TiO_2 nanoparticles, and a HTO−TiO_2 mixture, were used in the solid-state reaction for the synthesis of $Bi_{0.5}Na_{0.5}TiO_3$ (BNT) particles. In the synthesis of the BNT powder from the HTO titanium source, HTO (0.005 mol of Ti) and a stoichiometric ratio of Bi_2O_3 and Na_2CO_3 (Bi/Na/Ti mole ratio = 0.5:0.5:1) in the solvent of ethanol were mixed by ball milling with 5-mm-diameter zirconia balls for 24 h at a rotational speed of 60 rpm. The mixture was dried at 60 °C for 6 h and then heated at a desired temperature for 3 h in air with a heating rate of 10 °C/min. Similarly, BNT powder samples were prepared using anatase TiO_2 nanoparticles or a mixture of HTO and anatase TiO_2 nanoparticles as the titanium source instead of the HTO titanium source. The mole ratio of titanium in the HTO−TiO_2 mixture was 4:6.

Preparation of Oriented BNT Ceramic Materials. The starting materials of Bi_2O_3 (0.0125 mol), Na_2CO_3, HTO, and anatase TiO_2 powders were thoroughly mixed according to the BNT stoichiometric ratio, where the titanium mole ratio of HTO−TiO_2 was 4:6. This well-mixed starting material powder with solvent (3 g, 60 vol % toluene−40 vol % ethanol), binder [0.08 g, poly(vinylbutyral)], and plasticizer (74 μL, di-*n*-butyl phthalate) was milled by ball milling with 5-mm-diameter zirconia balls at a rotational speed of 60 rpm for 48 h. The resultant slurry was cast on a poly(ethylene terephthalate) (PET) film tape to form a green sheet using an auto film applicator (Tester Sangyo, PI-1210 filmcoater) by a doctor blade technique.[56] After drying, the green sheet was stacked into 64 layers with a size of 12 mm × 12 mm and then pressed at 20 MPa for 3 min at room temperature to form a green compact with a thickness of about 2 mm. Finally, the green compact was sintered with a desired temperature for 3 h in air with a heating rate of 10 °C/min.

Physical Characterization. The structures of powder and ceramic samples were investigated using a powder X-ray diffractometer (Shimadzu, XRD-6100) with Cu Kα (λ = 0.15418 nm) radiation. The size and morphology of the samples were observed using scanning electron microscopy (SEM; JEOL JSM-5500S) or field-emission

dx.doi.org/10.1021/ic4015256 | Inorg. Chem. 2013, 52, 10542−10551

scanning electron microscopy (FE-SEM; Hitachi S-900). Transmission electron microscopy (TEM) observation and selected-area electron diffraction (SAED) were performed on a JEOL model JEM-3010 system at 300 kV, and the powder sample was supported on a microgrid. Energy-dispersive spectroscopy (EDS; JEOL JED-2300T) was measured on the TEM system. The degrees of orientation (Lotgering factor, F) of the ceramic samples in the [100] direction were evaluated from the diffraction peak density of XRD in the range of 3−60° using Lotgering's formula[57]

$$F = \frac{P - P_0}{1 - P_0}, \quad P = \frac{\sum I(h00)}{\sum I(hkl)}, \quad P_0 = \frac{\sum I_0(h00)}{\sum I_0(hkl)}$$

where I and I_0 are the intensities of the (hkl) peaks for the oriented and unoriented samples, respectively. The BNT powder sample prepared using TiO_2 as a titanium source was used as the unoriented standard for evaluating the P_0 value. The density of the sintered compact was determined by a specific gravity measurement kit (Shimadzu SMK-401) with Archimedes' principle. The theoretical density of 5.997 g/cm^3 of BNT was used in the relative density calculation.[30,47]

RESULTS AND DISCUSSION

Formation of BNT Mesocrystals in a HTO−Bi_2O_3−Na_2CO_3 Reaction System. Figure 1 shows the X-ray diffraction (XRD) patterns of the powder samples obtained by the heat treatment of a HTO−Bi_2O_3−Na_2CO_3 mixture with the stoichiometric ratio of BNT. The diffraction peaks of the HTO, Na_2CO_3, and Bi_2O_3 phases were observed before heat treatment (Figure 1a). After heat treatment at 500 °C, in addition to the small amounts of the unreacted HTO, Na_2CO_3, and Bi_2O_3 phases, new phases of $Bi_{12}TiO_{20}$ (JCPDS File No. 34-0097) and BNT (JCPDS File No. 89-3109) were formed (Figure 1b), suggesting the partial reaction of the HTO−Bi_2O_3−Na_2CO_3 mixture. The basal spacing of HTO decreased from 0.870 to 0.732 nm because of dehydration of its interlayer water. At 600 °C, all of the starting HTO, Bi_2O_3, and Na_2CO_3 phases were reacted, and the product containing the BNT main phase and a very small amount of the $Bi_{12}TiO_{20}$ phase was formed. Although the crystal structure of BNT is rhombohedral, the diffraction lines are indexed based on the pseudocubic unit cell because of small rhombohedral distortion and can be identified by JCPDS File No. 89-3109 (cubic symmetry).[3,31,23,35,58,59] Only the BNT phase was obtained above 700 °C. Formation of the TiO_2 phase was not observed in all of the reaction temperature ranges studied here, suggesting that the HTO phase was transformed directly into the $Bi_{12}TiO_{20}$ or BNT phase in the reaction system. Formation of the BNT phase occurred at much lower temperature in the HTO−Bi_2O_3−Na_2CO_3 reaction system than in the normal TiO_2−Bi_2O_3−Na_2CO_3 reaction system (see the next section) because of the high reactivity of HTO.

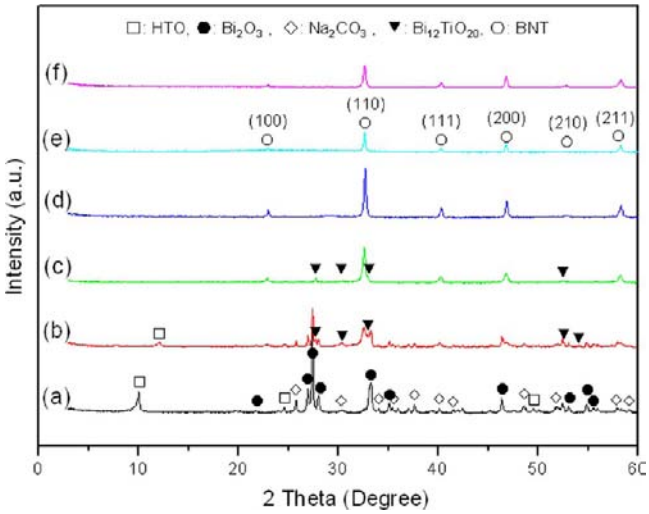

Figure 1. XRD patterns of the HTO−Na_2CO_3−Bi_2O_3 mixture (a) before and after heat treatment at (b) 500, (c) 600, (d) 700, (e) 800, and (f) 900 °C for 3 h, respectively.

The above results indicate that, in the HTO−Bi_2O_3−Na_2CO_3 reaction system, first the intermediate $Bi_{12}TiO_{20}$ phase is formed by reacting HTO with Bi_2O_3 (reaction 1), and then the intermediate product reacts with Na_2CO_3 and HTO (reaction 2), resulting in formation of the BNT phase.

$$6Bi_2O_3 + \frac{1}{1.73}H_{1.07}Ti_{1.73}O_4 \cdot nH_2O \rightarrow Bi_{12}TiO_{20} + xH_2O \quad (1)$$

$$Bi_{12}TiO_{20} + 6Na_2CO_3 + \frac{23}{1.73}H_{1.07}Ti_{1.73}O_4 \cdot nH_2O \rightarrow 24Bi_{0.5}Na_{0.5}TiO_3(BNT) + 6CO_2 + yH_2O \quad (2)$$

Figure 2 presents FE-SEM images of the HTO−Bi_2O_3−Na_2CO_3 mixtures before and after heat treatment. The platelike particle morphology of HTO with about 200 nm thickness and about 2 μm width can be observed in the HTO−Bi_2O_3−Na_2CO_3 mixture before heat treatment. This result indicates that HTO particle morphology has not been damaged during the ball-milling treatment. The platelike particles remained in its morphology after heat treatment at 500 °C (Figure 2b). It is interesting to observe some smaller holes with diameter of about 60 nm and cracks in the plate (Figure S1a in the Supporting Information, SI).

After heat treatment at 600 °C, the platelike particle morphology also remained, but the holes and cracks disappeared in platelike particles (Figure 2c). The platelike particle is constructed from nanoparticles with a size of about 100 nm. This result suggests that the polycrystalline platelike BNT particles are formed by an in situ topotactic reaction mechanism. The platelike particles collapsed, and blocklike particles with a size of about 200 nm were formed at 700 °C (Figure 2d). With increasing heat-treatment temperature to 800 and 900 °C, the sizes of the blocklike particles grow to about 400 and 800 nm, respectively (Figure 2e,f).

The formation reaction of BNT in the HTO−Bi_2O_3−Na_2CO_3 system was also investigated using TEM, high-resolution TEM (HRTEM), and SAED, and the results for the sample obtained at 600 °C are shown in Figure 3. The platelike particle is constructed from nanoparticles with a size of about 100 nm (Figure 3a), which is consistent with the FE-SEM result (Figure 2c). The fast-Fourier-transform (FFT)-filtered TEM image indicates that the nanoparticles with a size of about 100 nm correspond to the BNT cubic phase, where the fringe spacings of 3.90 and 2.80 Å correspond to (001) and (011) facets, respectively, and the angle between the (001) and (011) facets is 45°. Except the BNT nanoparticles of 100 nm, some small spherical nanoparticles with a size of about 5 nm were also observed on the surface of the platelike particle (Figure 3c). These small nanoparticles correspond to the $Bi_{12}TiO_{20}$ phase, which shows a fringe spacing of 3.19 Å matching with the (310) facet.

dx.doi.org/10.1021/ic4015256 | Inorg. Chem. 2013, 52, 10542−10551

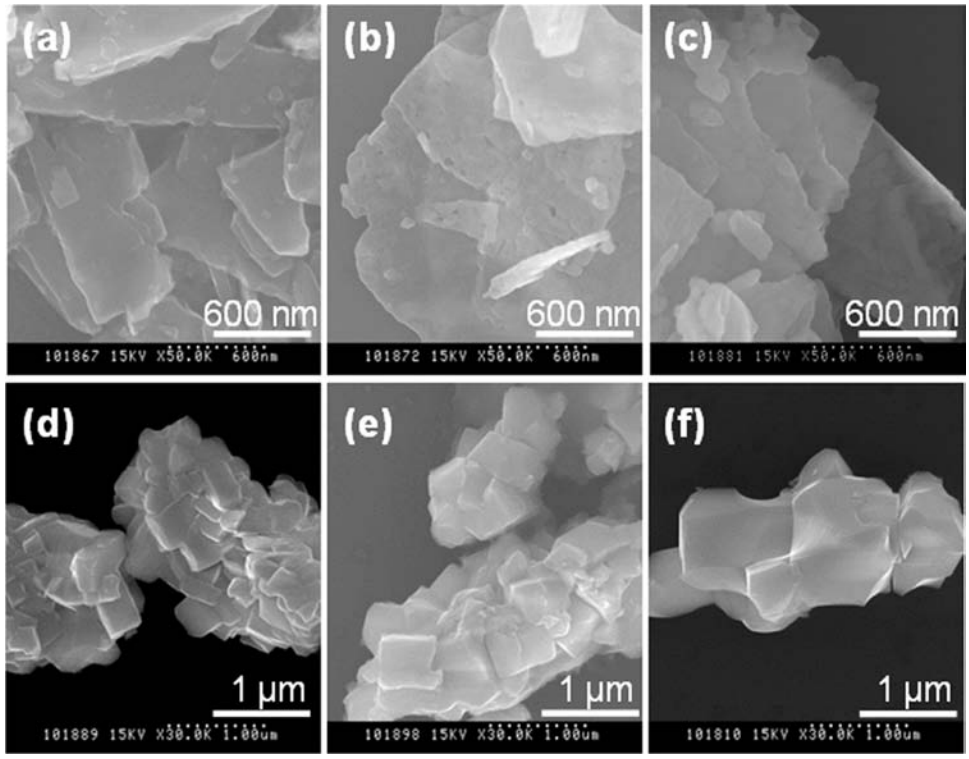

Figure 2. FE-SEM images of the HTO−Na_2CO_3−Bi_2O_3 mixture before (a) and after heat treatment at (b) 500, (c) 600, (d) 700, (e) 800, and (f) 900 °C for 3 h, respectively.

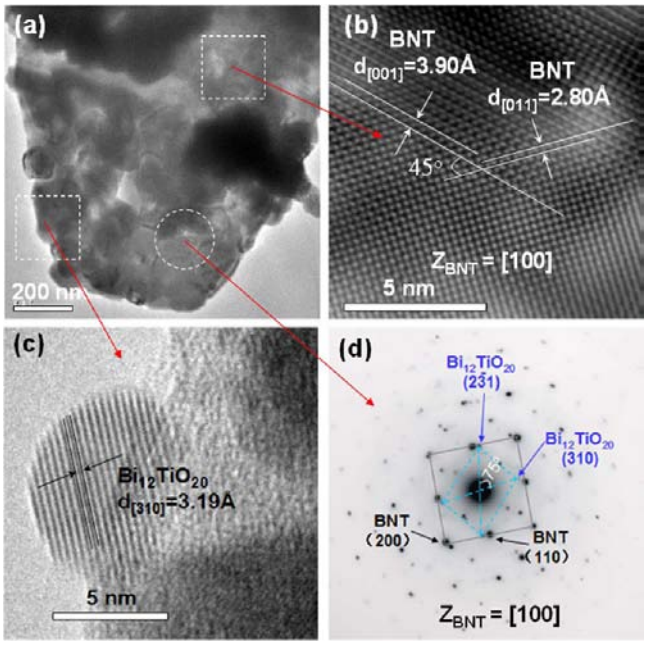

Figure 3. (a) TEM image, (b) FFT-filtered TEM image, (c) HRTEM image, and (d) SAED pattern of the sample obtained after heat treatment of a HTO−Na_2CO_3−Bi_2O_3 mixture at 600 °C for 3 h.

It is notable that two sets of SAED spots corresponding to the BNT perovskite and $Bi_{12}TiO_{20}$ phases are observed simultaneously in one platelike particle (Figure 3d), suggesting that the BNT and $Bi_{12}TiO_{20}$ phases coexist in one platelike particle. This result is consistent with the XRD result in Figure 2c. The SAED result reveals that all of the BNT nanoparticles and all of the $Bi_{12}TiO_{20}$ nanoparticles in one platelike particle show the same crystal-axis orientation directions, because they show diffraction spot patterns similar to their single-crystal diffraction spot patterns. Furthermore, the polycrystalline platelike BNT particle shows a [100]-axis orientation, and the basal plane of the platelike particle corresponds to the (100) facet that is vertical to the [100] orientation. These results reveal that reactions 1 and 2 in the formation process of BNT from HTO are in situ topotactic reactions, which result in the formation of [100]-oriented platelike BNT mesocrystals. The [100]-direction orientation of the BNT platelike mesocrystal is different from the [110]-direction orientation of the platelike $BaTiO_3$,[50] $Ba_{0.9}Ca_{0.1}TiO_3$,[19] and $Ba_{0.5}Bi_{0.5}K_{0.5}TiO_3$[51] mesocrystals prepared from the HTO precursor by solvothermal reactions.

It has been reported that platelike BNT single crystals with [100]-direction orientation can be prepared by molten-salt reactions using $Bi_4Ti_3O_{12}$[35,37] and $Na_{0.5}Bi_{4.5}Ti_4O_{15}$[3,31] layered compounds as the precursor over 900 °C. The reaction temperature is higher than that of the formation of platelike BNT mesocrystals using the HTO precursor because of the lower reactivities of the $Bi_4Ti_3O_{12}$ and $Na_{0.5}Bi_{4.5}Ti_4O_{15}$ precursors. In the molten-salt processes, first the Bi_2O_2(II) layer-structured $Bi_4Ti_3O_{12}$ and $Na_{0.5}Bi_{4.5}Ti_4O_{15}$ platelike particles were synthesized as precursors by molten-salt reactions, and then the platelike particles were reacted with Na_2CO_3 and TiO_2 to transform to the perovskite structure through topochemical conversion.[35,37] Although a possible transformation mechanism from the layered structure to the perovskite structure has been proposed, it is not very clear yet.[31,35]

On the basis of the results described above, we can give a schematic representation for the formation reaction mechanism of the [100]-oriented platelike BNT mesocrystal in the HTO−Bi_2O_3−Na_2CO_3 solid-state reaction system, as shown in Figure

dx.doi.org/10.1021/ic4015256 | Inorg. Chem. 2013, 52, 10542−10551

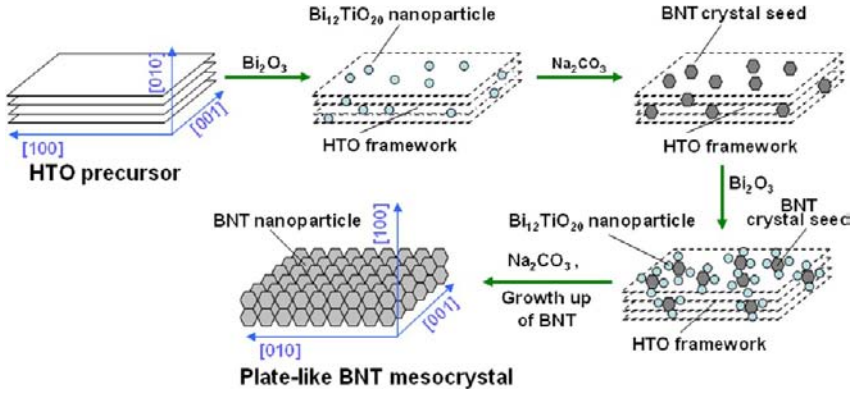

Figure 4. Reaction mechanism of the formation of platelike BNT mesocrystals in the HTO–Bi_2O_3–Na_2CO_3 solid-state reaction system.

4. In this reaction process, bismuth(III) species immigrate into the HTO bulk crystal through its interlayer pathway first and partially react with the TiO_6 octahedral layers of the HTO framework to form $Bi_{12}TiO_{20}$ nanoparticles in the HTO bulk crystal by the in situ structural transformation reaction. Then $Bi_{12}TiO_{20}$ nanoparticles react with TiO_6 octahedral layers and sodium(I) species in the bulk crystal to form BNT crystal seeds (nanoparticles). This reaction is also the in situ topotactic structural transformation reaction, and formed BNT crystal seeds show [100] orientation. In the next step, the bismuth(III) species sequentially reacts with the TiO_6 octahedral layers, which causes the formation of $Bi_{12}TiO_{20}$ nanoparticles on the BNT nanoparticle surface by a heteroepitaxial growth mechanism. Then $Bi_{12}TiO_{20}$ nanoparticles on the BNT nanoparticle surface react with the TiO_6 octahedral layers and sodium(I) species to grow BNT nanoparticles by an epitaxial growth mechanism.[60] Finally a [100]-oriented platelike BNT mesocrystal is obtained by consuming the HTO framework completely.

To give an exact relationship between the structures of the HTO precursor and BNT product, TEM and SAED studies were carried out on the HTO and partially reacted sample obtained at 500 °C (Figure 5). The platelike HTO particle is a single crystal with a smooth particle surface, and the basal plane of the platelike particle corresponds to the (010) facet. After heat treatment at 500 °C, the smooth particle surface changed to a rough surface. Three sets of SAED spots for the HTO-layered, the perovskite BNT, and the $Bi_{12}TiO_{20}$ intermediate phases are observed simultaneously in one platelike particle, indicating that the HTO, BNT, and $Bi_{12}TiO_{20}$ phases coexist in one platelike particle. In one platelike particle, the HTO axis directions of [010], [002], and [100] correspond to the BNT axis directions of [100], [001], and [010], respectively, suggesting that a three-dimensional topotactic reaction occurs in the structural transformation process. That is, there is a specific relationship between the structures of the HTO precursor and BNT product in the in situ topotactic structure transformation process, where (010), (001), and (100) facets of the layered HTO structure are converted to (100), (001), and (010) facets of the BNT perovskite structure, respectively (Figure 6).

Formation of BNT in the TiO_2–Bi_2O_3–Na_2CO_3 Reaction System. The normal TiO_2–Bi_2O_3–Na_2CO_3 solid-state reaction system was also investigated in order to compare with the HTO–Bi_2O_3–Na_2CO_3 reaction system. Figure 7 shows the XRD patterns of the samples obtained by heat treatment of a TiO_2–Bi_2O_3–Na_2CO_3 mixture with the stoichiometric ratio of

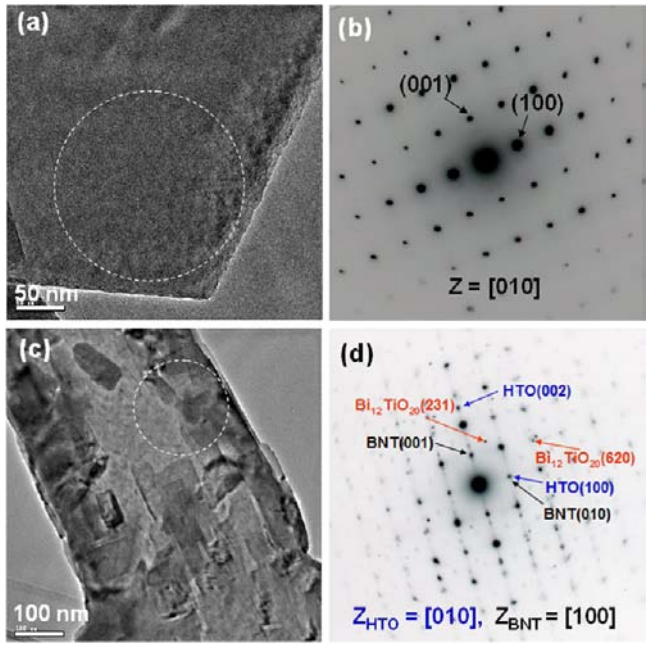

Figure 5. (a and c) TEM images and (b and d) SAED patterns of (a and b) HTO and (c and d) platelike particle obtained by the heat treatment of a HTO–Na_2CO_3–Bi_2O_3 mixture at 500 °C for 3 h.

BNT. The diffraction peaks of the TiO_2, Na_2CO_3, and Bi_2O_3 phases were observed before heat treatment (Figure 7a). At 700 °C, all of the starting TiO_2, Bi_2O_3, and Na_2CO_3 phases were transformed into the intermediates of tetragonal $Bi_4Ti_3O_{12}$ (JCPDS File No. 47-0398) and cubic $Bi_{12}TiO_{20}$ (JCPDS File No. 34-0097).[61] Most of the intermediates $Bi_4Ti_3O_{12}$ and $Bi_{12}TiO_{20}$ were transformed into the BNT phase at 800 °C, and only the BNT phase was obtained above 900 °C. These results indicate that a higher heat-treatment temperature is necessary for the formation of BNT in the normal TiO_2–Bi_2O_3–Na_2CO_3 reaction system than in the HTO–Bi_2O_3–Na_2CO_3 topotactic reaction system (Figure 1). Although HTO has a much larger particles size, it shows a higher reactivity in the BNT formation reaction than anatase TiO_2 nanoparticles.

The SEM study indicates that the products obtained at 700 and 800 °C show mainly spherical particle morphologies with a small amount of rodlike particles (see Figure S2 in the SI). The rodlike particles may correspond to the $Bi_4Ti_3O_{12}$ phase.[62,63] The BNT product obtained at 900 °C shows a square block

dx.doi.org/10.1021/ic4015256 | Inorg. Chem. 2013, 52, 10542–10551

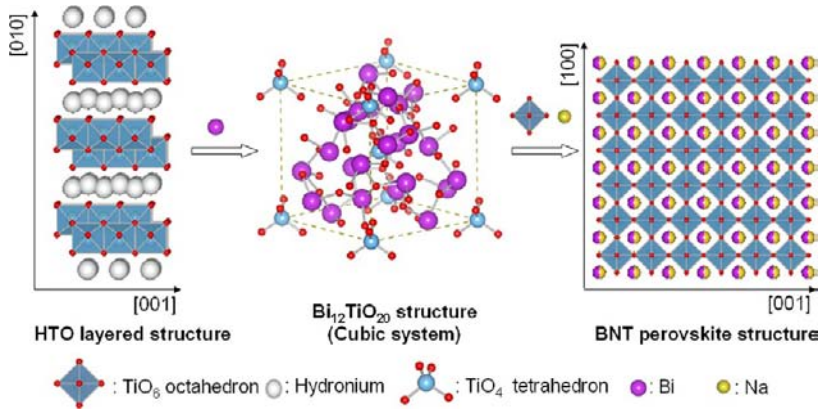

Figure 6. Schematic illustration of crystal structural evolution from HTO to BNT in an in situ topotactic transformation for the HTO–Na_2CO_3–Bi_2O_3 reaction system.

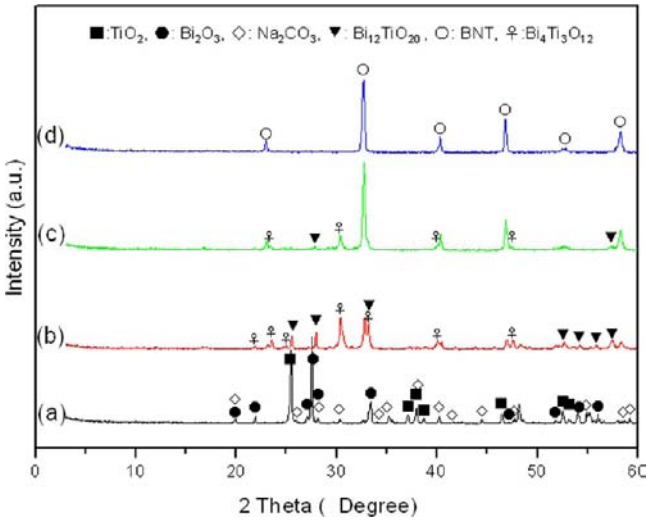

Figure 7. XRD patterns of the TiO_2–Na_2CO_3–Bi_2O_3 mixture (a) before and after heat treatment at (b) 700, (c) 800, and (d) 900 °C for 3 h, respectively.

morphology with a size of about 5 μm. The particle size of the product increases with increasing heat-treatment temperature.

Formation of the intermediates $Bi_4Ti_3O_{12}$ and $Bi_{12}TiO_{20}$ in the normal TiO_2–Bi_2O_3–Na_2CO_3 solid-state reaction system for synthesis of the BNT phase has been also reported.[64,65] In this reaction system, first $Bi_{12}TiO_{20}$ is formed by reaction 3, then $Bi_{12}TiO_{20}$ is transformed to $Bi_4Ti_3O_{12}$ by reaction 4,[65] and finally $Bi_4Ti_3O_{12}$ is transformed to BNT by reaction 5,[23,30] as follows:

$$6Bi_2O_3 + TiO_2 \rightarrow Bi_{12}TiO_{20} \quad (3)$$

$$Bi_{12}TiO_{20} + 8TiO_2 \rightarrow 3Bi_4Ti_3O_{12} \quad (4)$$

$$Bi_4Ti_3O_{12} + 2Na_2CO_3 + 5TiO_2 \rightarrow 8Bi_{0.5}Na_{0.5}TiO_3(BNT) + 2CO_2 \quad (5)$$

This is different from reactions 1 and 2, where there is no formation of the intermediate $Bi_4Ti_3O_{12}$ in the HTO–Bi_2O_3–Na_2CO_3 topotactic reaction system. This fact can be explained by differences in the intermediate $Bi_{12}TiO_{20}$ formation mechanism in these two reaction systems. In the HTO–Bi_2O_3–Na_2CO_3 reaction system, formation of the intermediate $Bi_{12}TiO_{20}$ nanoparticles occurs on the BNT crystal seed surface in the HTO crystal bulk where there is enough titanium(IV) source for the formation of BNT. Therefore, the $Bi_{12}TiO_{20}$ nanoparticles show a high reactivity and can be transformed directly to BNT by the epitaxial growth mechanism, as shown in Figure 4. On the other hand, in the TiO_2–Bi_2O_3–Na_2CO_3 solid-state reaction system, formation of the intermediate $Bi_{12}TiO_{20}$ occurs on the interface between TiO_2 and Bi_2O_3 particle surfaces. The intermediate $Bi_{12}TiO_{20}$ cannot be transformed directly to BNT because there is not enough titanium(IV) source. A two-step reaction is necessary to provide enough titanium(IV) source. First, the intermediate $Bi_{12}TiO_{20}$ reacts with TiO_2 to form another intermediate $Bi_4Ti_3O_{12}$ by reaction 4, and then the intermediate $Bi_4Ti_3O_{12}$ reacts with TiO_2 and Na_2CO_3 to form the final product BNT.

Formation of BNT Mesocrystals in the HTO–TiO_2–Bi_2O_3–Na_2CO_3 Reaction System. We also studied the formation of BNT in the HTO–TiO_2–Bi_2O_3–Na_2CO_3 reaction system, where both HTO and TiO_2 nanoparticles were used as titanium sources, because high degree of orientation and high-density BNT ceramic materials can be prepared using this reaction system (see the next section). We chose the mole ratio of HTO/TiO_2 = 4:6 in the HTO–TiO_2–Bi_2O_3–Na_2CO_3 reaction system because such a condition is suitable for the fabrication of high degree of orientation ceramic materials.[23,30] Before heat treatment, the diffraction peaks of the HTO, TiO_2, Na_2CO_3, and Bi_2O_3 phases were observed (Figure 8a). After heat treatment at 500 °C, in addition to the dehydrated HTO, TiO_2, Na_2CO_3, and Bi_2O_3 phases, the intermediate $Bi_{12}TiO_{20}$ and BNT phases were also observed (Figure 8b), suggesting the partial reaction of the HTO–TiO_2–Bi_2O_3–Na_2CO_3 mixture. Because the peak intensity of TiO_2 did not change, it can be concluded that TiO_2 did not take part in the reaction at this reaction temperature. The basal spacing of HTO also decreased from 0.870 to 0.732 nm because of dehydration of the interlayer water.

At 600 °C, all starting Bi_2O_3, Na_2CO_3, HTO, TiO_2 phases were reacted, and the product containing the BNT main phase and a small amount of the $Bi_{12}TiO_{20}$ phase was formed (Figure 8c). Only BNT phase was obtained above 700 °C (Figure 8d–f). These results are similar to those of the HTO–Bi_2O_3–Na_2CO_3 reaction system (Figure 1), which is different from the TiO_2–Bi_2O_3–Na_2CO_3 system (Figure 7). The BNT phase can be formed at low temperature (700 °C) without the formation of intermediate $Bi_4Ti_3O_{12}$ in the HTO–TiO_2–Bi_2O_3–Na_2CO_3 reaction system. The full width at half-maximum of the BNT

dx.doi.org/10.1021/ic4015256 | Inorg. Chem. 2013, 52, 10542–10551

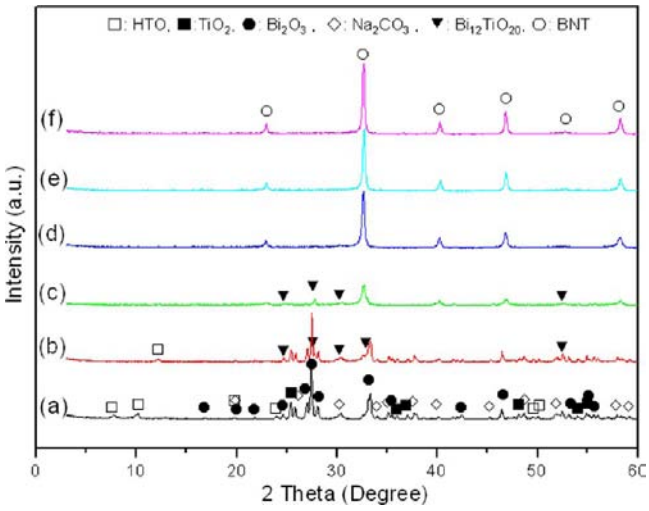

Figure 8. XRD patterns of the HTO−TiO_2−Bi_2O_3−Na_2CO_3 mixture (a) before and after heat treatment at (b) 500, (c) 600, (d) 700, (e) 800, and (f) 900 °C, respectively. The titanium mole ratio of HTO/TiO_2 = 4:6.

phase obtained from the HTO−TiO_2−Bi_2O_3−Na_2CO_3 reaction system (0.448°) was larger than that from the HTO−Bi_2O_3−Na_2CO_3 reaction system (0.292°) at 600 °C. This result reveals that the HTO−Bi_2O_3−Na_2CO_3 reaction system has higher reactivity and gives a higher crystallinity of the BNT phase than the HTO−TiO_2−Bi_2O_3−Na_2CO_3 reaction system.

The FE-SEM results reveal that HTO shows platelike morphology before heat treatment in the HTO−TiO_2−Bi_2O_3−Na_2CO_3 mixture (Figure 9). The platelike particles and small nanoparticles were observed in the sample after heat treatment at 500 °C, and some fissures were formed on the platelike particles (Figure S1b in the SI). The nanoparticles correspond to the unreacted TiO_2, Bi_2O_3, and Na_2CO_3. After heat treatment in a temperature range of 600−800 °C, the unreacted TiO_2, Bi_2O_3, and Na_2CO_3 nanoparticles disappeared and were fused into the platelike particles, while the platelike particles grow to the larger platelike particles. The larger platelike particle is constructed from nanoparticles with a size of about 150 nm, which is larger than the nanoparticles (100 nm) in the platelike BNT particle prepared in the HTO−Bi_2O_3−Na_2CO_3 reaction system. This result suggests that a mass-transport process from the TiO_2 nanoparticles to the platelike particles occurs, resulting in crystal growth on the platelike BNT particle in this temperature range. When the heat-treatment temperature was reached at 900 °C, the platelike particle collapsed into small particles with a size of 300 nm, which is similar to that of the HTO−Bi_2O_3−Na_2CO_3 reaction system.

In order to understand the formation reaction of the BNT phase in the HTO−TiO_2−Bi_2O_3−Na_2CO_3 reaction system, the obtained samples were also investigated using TEM and SAED (Figure 10). The platelike particle prepared at 600 °C shows two sects of diffraction spot patterns that are similar to the single crystals. One corresponds to the BNT phase and the other to the $Bi_{12}TiO_{20}$ phase. The BNT nanoparticles in a platelike particle show the same orientation as the [100] direction because of formation of the [100]-oriented BNT mesocrystal. This result is also similar to that of the HTO−Bi_2O_3−Na_2CO_3 reaction system at 600 °C (Figure 3d). The TEM image of the sample prepared at 700 °C also presents a platelike morphology, but it is thicker than the platelike BNT mesocrystal prepared in the HTO−Bi_2O_3−Na_2CO_3 reaction system, where the nanoparticles constructing the platelike mesocrystal are not observed clearly (Figure 10c). This is

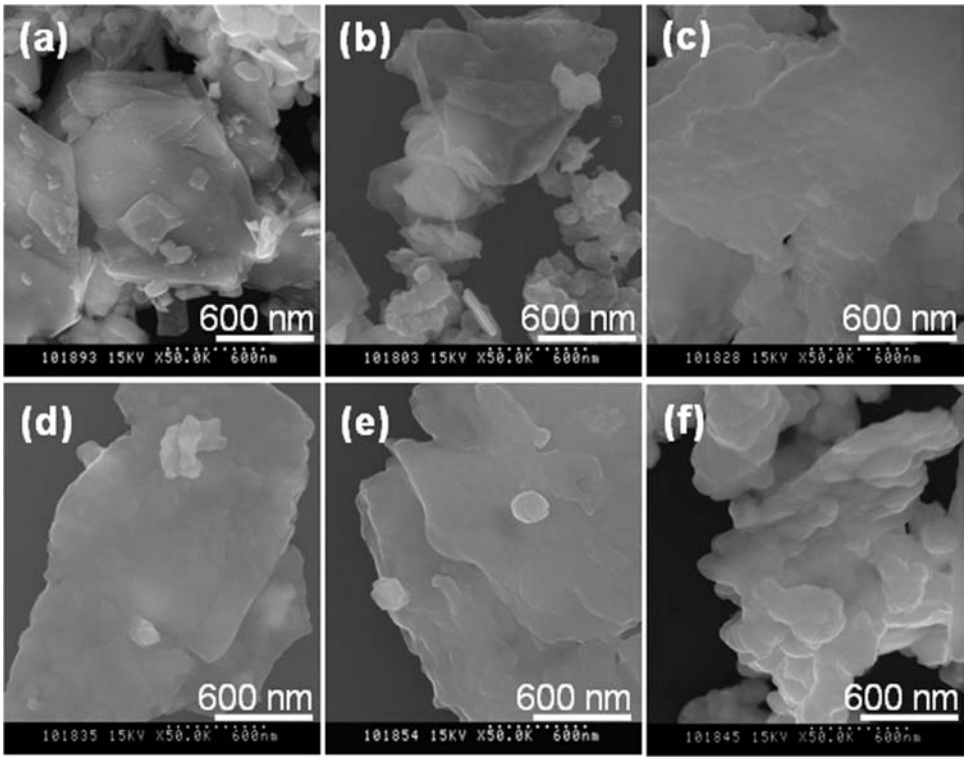

Figure 9. FE-SEM images of the HTO−TiO_2−Bi_2O_3−Na_2CO_3 mixture (a) before and after heat treatment at (b) 500, (c) 600, (d) 700, (e) 800, and (f) 900 °C, respectively. The titanium mole ratio of HTO/TiO_2 = 4:6.

dx.doi.org/10.1021/ic4015256 | Inorg. Chem. 2013, 52, 10542−10551

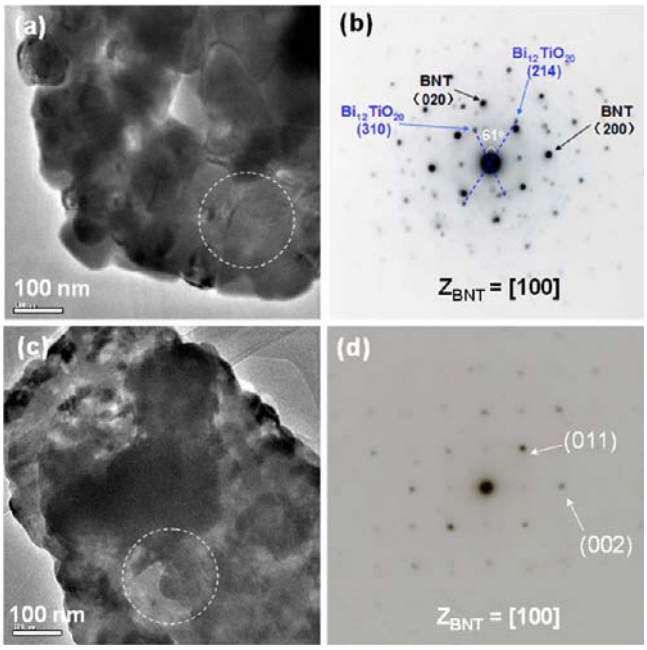

Figure 10. (a and c) TEM images and (b and d) SAED patterns of the samples obtained by heat treatment of the HTO−TiO_2−Na_2CO_3−Bi_2O_3 mixture at (a and b) 600 and (c and d) 700 °C for 3 h, respectively.

because the platelike mesocrystal is too thick to be transmitted by the electron beam of the TEM system. The platelike BNT mesocrystal retained the [100] orientation and shows the single-crystal SAED pattern after heat treatment at 700 °C, although it grows. EDS analysis on the platelike BNT mesocrystal indicated that the platelike mesocrystal shows a homogeneous chemical composite distribution with an average mole ratio of Bi/Na/Ti = 0.48:0.48:1.0 (see Figure S3 in the SI), which is in good accordance with the designed composition of BNT. This result reveals that crystal growth of the [100]-oriented platelike BNT mesocrystal via a mass-transport process occurs by the epitaxial growth mechanism.

On the basis of the results described above, a reaction mechanism of formation of the [100]-oriented platelike BNT mesocrystal in the HTO−TiO_2−Bi_2O_3−Na_2CO_3 solid-state reaction is given in Figure 11. In the first step of the reaction, the platelike HTO particles react with Na_2CO_3 and Bi_2O_3 to form the platelike BNT mesocrystal by an in situ topotactic reaction similar to the case in the HTO−Bi_2O_3−Na_2CO_3 reaction system, as shown in Figure 4, because HTO shows higher reactivity in the formation reaction of the BNT phase than that of the TiO_2 nanoparticles. This reaction is almost completed at 600 °C, and the platelike BNT mesocrystal constructed from [100]-oriented nanoparticles is formed. In the second step of the reaction, TiO_2 nanoparticles react with Na_2CO_3 and Bi_2O_3 to form the BNT phase on the platelike BNT mesocrystal surface by an epitaxial crystal growth mechanism. Epitaxial growth can lower the reaction temperature for formation of the BNT phase from the TiO_2−Bi_2O_3−Na_2CO_3 reaction system. This is the reason why formation of the BNT phase can be completed in the HTO−TiO_2−Bi_2O_3−Na_2CO_3 reaction system at lower temperature (700 °C) than that in the TiO_2−Bi_2O_3−Na_2CO_3 reaction system (900 °C). Epitaxial growth of the BNT phase on the platelike mesocrystal surface accompanies consumption of the unreacted TiO_2, Na_2CO_3, and Bi_2O_3 in the reaction system and fusion of these particles into the platelike mesocrystals by the mass-transport process. In the epitaxial growth process, the [100]-oriented BNT nanoparticles in the platelike mesocrystal act as crystal seeds; namely, the oriented nanoparticles grew up and kept their [100] orientation. This is the reason why the larger [100]-oriented platelike BNT mesocrystal can be formed in the HTO−TiO_2−Bi_2O_3−Na_2CO_3 reaction system.

Fabrication of BNT Oriented Ceramic Materials. We tried to fabricate BNT oriented ceramic materials using both the HTO−Bi_2O_3−Na_2CO_3 and HTO−TiO_2−Bi_2O_3−Na_2CO_3 reaction systems by the RTGG method. Figure 12 presents the XRD patterns of the ceramic materials obtained by sintering the green compacts prepared by the tape-casting method with the HTO−Bi_2O_3−Na_2CO_3 and HTO−TiO_2−Bi_2O_3−Na_2CO_3 mixtures, respectively. All of the sintered materials show a relatively higher peak intensity of the (h00) plane, indicating that [100]-

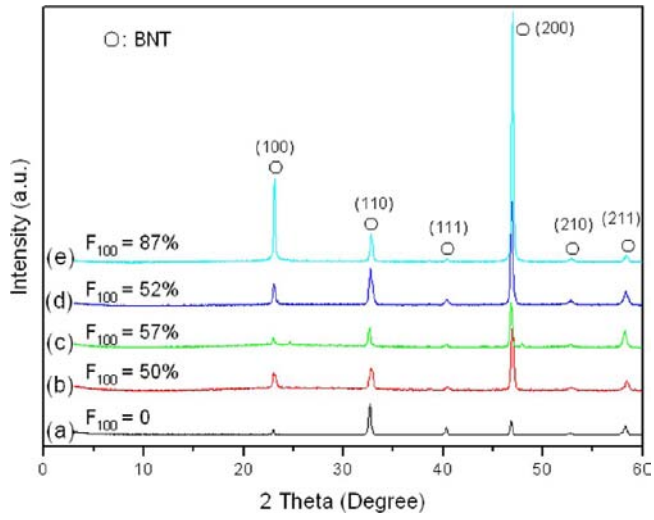

Figure 12. XRD patterns of (a) the BNT powder sample obtained by sintering the TiO_2−Bi_2O_3−Na_2CO_3 mixture at 1100 °C for 3 h and the BNT ceramic samples obtained by sintering (b and d) the HTO−Bi_2O_3−Na_2CO_3 green compact and (c and e) the HTO−TiO_2−Bi_2O_3−Na_2CO_3 green compact at (b and c) 1000 and (d and e) 1100 °C for 3 h, respectively.

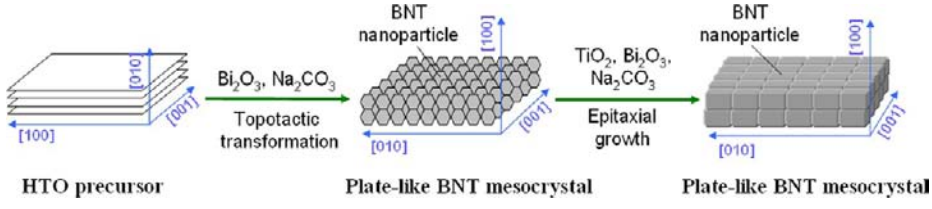

Figure 11. Reaction mechanism of formation of the platelike BNT mesocrystal in the HTO−TiO_2−Bi_2O_3−Na_2CO_3 solid-state reaction.

dx.doi.org/10.1021/ic4015256 | Inorg. Chem. 2013, 52, 10542−10551

oriented ceramic materials can be fabricated using the platelike HTO particles as the template. The degree of orientation (Lotgering factor, F) increases with increasing sintering temperature from 1000 to 1100 °C. The BNT ceramic materials fabricated with the HTO−TiO_2−Bi_2O_3−Na_2CO_3 reaction system show a higher degree of orientation than thoset with the HTO−Bi_2O_3−Na_2CO_3 reaction system. The highest orientation degree of 87% can be achieved using the HTO−TiO_2−Bi_2O_3−Na_2CO_3 reaction system. This orientation degree value is higher than those fabricated with $Bi_4Ti_3O_{12}$ (79%)[30] and $Na_{0.5}Bi_{4.5}Ti_4O_{15}$ (55%)[31] as the templates.

Figure 13 shows the SEM images of the surface microstructures of the ceramic samples fabricated by sintering green

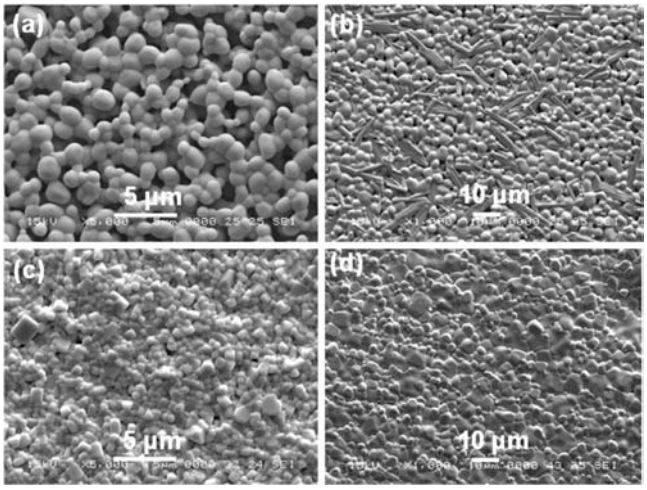

Figure 13. SEM images of ceramic samples obtained by sintering the HTO−Bi_2O_3−Na_2CO_3 green compact at (a) 1000 and (b) 1100 °C and by heat treatment of the HTO−TiO_2−Bi_2O_3−Na_2CO_3 green compact at (c) 1000 and (d) 1100 °C for 3 h, respectively.

compacts. In the HTO−Bi_2O_3−Na_2CO_3 reaction system, a porous ceramic sample with a grain size of about 2 μm was obtained at 1000 °C. After sintering at 1100 °C, the ceramic sample constructed from the spherical grains with a size of about 5 μm diameter and rodlike grains with a size of about 3 μm diameter and 10 μm length was obtained. The rodlike grains may be assigned to the $Bi_4Ti_3O_{12}$ that has a rodlike morphology.[66,67] Formation of the $Bi_4Ti_3O_{12}$ phase is due to vaporization of sodium species from the sample surface at high temperature. The density measurement result indicates that this ceramic material has a relative density of 85%. In the HTO−TiO_2−Bi_2O_3−Na_2CO_3 reaction system, however, a ceramic sample with higher relative density and a uniform grain size of about 1 μm was obtained after sintering at 1000 °C. After sintering at 1100 °C, the grain size of the ceramic sample increased to about 2 μm, and a high-density (96%) ceramic sample was obtained. This relative density is much higher than that (86%) fabricated with $Bi_4Ti_3O_{12}$ as the template.[58]

The above sintering results demonstrate that the HTO−TiO_2−Bi_2O_3−Na_2CO_3 reaction system is suitable for fabrication of the BNT oriented ceramic materials, and a high [100]-oriented BNT ceramic sample with high density and small grain size can be obtained. The success on the fabrication of a high-density BNT oriented ceramic gives us an opportunity to study its piezoelectricity. A preliminary piezoelectric study reveals that the BNT ceramic sample shows a ferroelectric polarization−electric field (P−E) loop with a remnent polarization (P_r) of 30 μC/cm^2 and a coercive field (E_c) of 65 kV/cm. The apparent piezoelectric constant d_{33}* value estimated from a unipolar strain−electric field (S−E) curve is about 98 pC/N, which is larger than 74 pC/N reported for the BNT nonoriented ceramics.[68] The d_{33}* value may be further enhanced after optimization of the measurement conditions and the detailed piezoelectric study is carried out. This result suggests that the BNT oriented ceramic with small grain size is promising for the high-performance piezoelectric materials, where the both texture and domain engineering techniques can be applied simultaneously.[15]

CONCLUSIONS

The [100]-oriented platelike BNT mesocrystals can be prepared using the HTO−Bi_2O_3−Na_2CO_3 and HTO−TiO_2−Bi_2O_3−Na_2CO_3 reaction systems. The platelike BNT mesocrystals prepared by these methods are constructed from [100]-oriented BNT nanocrystals. The platelike BNT mesocrystals are formed by a topotactic structural transformation mechanism in the HTO−Bi_2O_3−Na_2CO_3 reaction system and by the combination mechanism of the topotactic structural transformation and epitaxial crystal growth in the HTO−TiO_2−Bi_2O_3−Na_2CO_3 reaction system. The HTO precursor shows high reactivity in the formation reaction of BNT, resulting in the formation of BNT at lower temperature than those with TiO_2 nanoparticles and layered compounds of $Bi_4Ti_3O_{12}$ and $Na_{0.5}Bi_{4.5}Ti_4O_{15}$ platelike particles as the precursors. The HTO−Bi_2O_3−Na_2CO_3 and HTO−TiO_2−Bi_2O_3−Na_2CO_3 reaction systems can be applied to the fabrication of [100]-oriented BNT ceramic materials. The BNT ceramic materials with a high degree of orientation, high density, and small grain size can be obtained using the HTO−TiO_2−Bi_2O_3−Na_2CO_3 reaction system.

ASSOCIATED CONTENT

Supporting Information

Additional experimental results as discussed in the text (Figures S1−S3). This material is available free of charge via the Internet at http://pubs.acs.org.

AUTHOR INFORMATION

Corresponding Author

*E-mail: feng@eng.kagawa-u.ac.jp. Tel: +81 (0)87-864-240. Fax: +81 (0)87-864-2402.

Present Address

⊥Q.F.: Department of Advanced Materials Science, Faculty of Engineering, Kagawa University, 2217-20 Hayashi-cho, Takamatsu-shi, 761-0396 Japan.

Notes

The authors declare no competing financial interest.

ACKNOWLEDGMENTS

We thank Prof. S. Wada of the University of Yamanashi for his help on the piezoelectric study. This work was supported in part by Grants-in-Aid for Scientific Research (B) (Grant 23350101) from Japan Society for the Promotion of Science and Kagawa University.

REFERENCES

(1) Aksel, E.; Jones, J. L. *Sensors* **2010**, *10*, 1935−1954.
(2) Saito, Y.; Takao, H.; Tani, T.; Nonoyama, T.; Takatori, K.; Homma, T.; Nagaya, T.; Nakamura, M. *Nature* **2004**, *432*, 84−87.

(3) Zeng, J. T.; Kwok, K. W.; Tam, W. K.; Tian, H. Y.; Jiang, X. P.; Chan, H. L. W. *J. Am. Ceram. Soc.* **2006**, *89*, 3850−3853.
(4) Safari, A.; Abazari, M. *IEEE Trans. Ultrason. Ferroelectr. Freq. Control* **2010**, *57*, 2165−2176.
(5) Smolenskii, G. A.; Isupov, V. A.; Agranovskaya, A. I.; Krainik, N. N. *Sov. Phys. Solid State (Engl. Transl.)* **1961**, *2*, 2651−2654.
(6) Jaffe, B.; Cook, W. R.; Jaffe, H. *Piezoelectric Ceramics*; Academic Press: London, 1971; p 1.
(7) Elkechai, O.; Manier, M.; Mercurio, J. P. *Phys. Status Solidi A* **1996**, *157*, 499−560.
(8) Dorcet, V.; Trolliard, G. A T. *Acta. Mater.* **2008**, *56*, 1753−1761.
(9) Trolliard, G.; Dorcet, V. *Chem. Mater.* **2008**, *20*, 5074−5082.
(10) Barick, B. K.; Choudhary, R. N. P.; Pradhan, D. K. *Mater. Chem. Phys.* **2012**, *132*, 1007−1014.
(11) Suchanicz, J. *J. Phys. Chem. Solids* **2001**, *62*, 1271−1276.
(12) Zuo, R. Z.; Su, S.; Wu, Y.; Fu, J.; Wang, M.; Li, L. T. *Mater. Chem. Phys.* **2008**, *110*, 311−315.
(13) Liao, Y. W.; Xiao, D. Q. *J. Mater. Sci. Technol.* **2009**, *25*, 777−780.
(14) Yang, J. N.; Liu, P.; Bian, X. B.; Jing, H. X.; Wang, Y. J.; Zhang, Y.; Wu, Y.; Song, W. H. *Mater. Sci. Eng., B* **2011**, *176*, 260−265.
(15) Wada, S.; Takeda, K.; Muraishi, T.; Kakemoto, H.; Tsurumi, T.; Kimura, T. *Ferroelectrics* **2008**, *373*, 11−21.
(16) Sabolsky, E. M.; Trolier-McKinstry, S.; Messing, G. L. *J. Appl. Phys.* **2003**, *93*, 4072−4080.
(17) Cao, W.; Randall, C. A. *J. Phys. Chem. Solids* **1996**, *57*, 1499−1505.
(18) Waanders, J. W. *Piezoelectric Ceramics: Properties and applications*; Philips Components: Eindhoven, The Netherlands, 1991; pp 41−64.
(19) Kong, X. G.; Ishikawa, Y.; Shinagawa, K.; Feng, Q. *J. Am. Ceram. Soc.* **2011**, *94*, 3716−3721.
(20) Wada, S.; Takeda, K.; Muraishi, T.; Kakemoto, H.; Tsurumi, T.; Kimura, T. *Jpn. J. Appl. Phys.* **2007**, *46*, 7039−7043.
(21) Takahashi, H.; Numamoto, Y.; Tani, J.; Tsurekawa, S. *Jpn. J. Appl. Phys.* **2006**, *45*, 7405−7408.
(22) Kimura, T. *J. Ceram. Soc. Jpn.* **2006**, *114*, 15−25.
(23) Kimura, T.; Takahashi, T.; Tani, T.; Saito, Y. *J. Am. Ceram. Soc.* **2004**, *87*, 1424−1429.
(24) Kimura, T.; Takahashi, T.; Tani, T.; Saito, Y. *Ceram. Int.* **2004**, *30*, 1161−1167.
(25) Wu, M. J.; Li, Y. X.; Wang, D.; Yin, Q. R. *Ceram. Int.* **2008**, *34*, 753−756.
(26) Xue, H.; Xiong, Z. X. *J. Alloys Compd.* **2009**, *467*, 338−341.
(27) Su, S.; Zuo, R. H.; Lv, D. Y.; Fu, J. *Powder Technol.* **2012**, *217*, 11−15.
(28) Soto, T.; Kimura, T. *Ceram. Int.* **2008**, *34*, 757−760.
(29) Sugawara, T.; Shimizu, M.; Kimura, T.; Takatori, K.; Tani, T. *Ceram. Trans.* **2003**, *136*, 389−406.
(30) Motohashi, T.; Kimura, T. *J. Eur. Ceram. Soc.* **2007**, *27*, 3633−3636.
(31) Setasuwon, P.; Kijamnajsuk, S. *Sci. Technol. Adv. Mater.* **2006**, *7*, 780−784.
(32) Kimura, T.; Motohashi, T. *Key Eng. Mater.* **2009**, *388*, 209−212.
(33) Roy, M.; Bala, I.; Barbar, S. K.; Jangid, S.; Dave, P. *J. Phys. Chem. Solids* **2011**, *72*, 1347−1353.
(34) Jovalekić, C.; Zdujić, M. *Ceram. Int.* **2010**, *36*, 789−792.
(35) Wu, M.; Li, Y. *Mater. Lett.* **2010**, *64*, 1157−1159.
(36) Setasuwon, P.; Kijamnajsuk, S. *Cryst. Eng. Commun.* **2009**, *11*, 1947−1950.
(37) Zhao, W.; Zhou, H. P.; Yan, Y. K.; Liu, D. *J. Am. Ceram. Soc.* **2008**, *91*, 1322−1325.
(38) Setasuwon, P.; Vaneesorn, N.; Kijamnajsuk, S.; Thanaboonsombut, A. *Sci. Technol. Adv. Mater.* **2005**, *6*, 278−281.
(39) Radha, V.; Vijayakumar, B.; Rama Devi, V.; Prasad, G.; Vithal, M. *Ceram. Int.* **2010**, *36*, 1485−1489.
(40) Lencka, M. M.; Oledzka, M.; Riman, R. E. *Chem. Mater.* **2000**, *12*, 1323−1330.
(41) Pookmanee, P.; Rujijanagul, G.; Ananta, S.; Heimann, R. B.; Phanichphant, S. *J. Eur. Ceram. Soc.* **2004**, *24*, 517−520.
(42) Jing, X. Z.; Li, Y. X.; Yin, Q. G. *Mater. Sci. Eng., B* **2003**, *99*, 506−510.
(43) Wang, Y. G.; Xu, G.; Yang, L. L.; Ren, Z. H.; Wei, X.; Weng, W. J.; Du, P. Y.; Shen, G.; Han, G. R. *Ceram. Int.* **2009**, *35*, 1657−1659.
(44) Kim, C. Y.; Sekino, T.; Niihara, K. *J. Am. Ceram. Soc.* **2003**, *86*, 1464−1467.
(45) Kanie, K.; Sakai, H.; Tani, J.; Takahashi, H.; Muramatsu, A. *Mater. Trans.* **2007**, *48*, 2174−2178.
(46) Khamman, O.; Watcharapasorn, A.; Pengpat, K.; Tunkasiri, T. *J. Mater. Sci.* **2006**, *41*, 5391−5394.
(47) Qi, J. Q.; Sun, L.; Du, P.; Li, L. T. *J. Am. Ceram. Soc.* **2010**, *93*, 1044−1048.
(48) Feng, Q.; Hirasawa, M.; Kajiyoshi, K.; Yanagisawa, K. *J. Am. Ceram. Soc.* **2005**, *88*, 1415−1420.
(49) Feng, Q.; Hirasawa, M.; Yanagisawa, K. *Chem. Mater.* **2001**, *13*, 290−296.
(50) Feng, Q.; Ishikawa, Y.; Makita, Y.; Yamamoto, Y. *J. Ceram. Soc. Jpn.* **2010**, *118*, 141−146.
(51) Kong, X. G.; Hu, D. W.; Ishikawa, Y.; Tanaka, Y.; Feng, Q. *Chem. Mater.* **2011**, *23*, 3978−3986.
(52) Zhou, L.; O'Brien, P. *Small* **2008**, *4*, 1566−1574.
(53) Cölfen, H.; Mann, S. *Angew. Chem., Int. Ed.* **2003**, *42*, 2350−2356.
(54) Ye, J. F.; Liu, W.; Cai, J. G.; Chen, S.; Zhao, X. W.; Zhou, H. H.; Qi, L. M. *J. Am. Chem. Soc.* **2011**, *133*, 933−940.
(55) Song, R. Q.; Cölfen, H. *Adv. Mater.* **2010**, *22*, 1301−1330.
(56) Mistler, R. E.; Twiname, E. R. *Tape Casting: Theory and Practice*; American Ceramic Society: Westerville, OH, 2000; pp 83−186.
(57) Lotgering, F. K. *J. Inorg. Nucl. Chem.* **1959**, *9*, 113−123.
(58) Fukuchi, E.; Kilnura, T. *J. Am. Ceram. Soc.* **2002**, *85*, 1461−1466.
(59) Chou, C. S.; Yang, R. Y.; Chen, J. H.; Chou, S. W. *Powder Technol.* **2010**, *199*, 264−271.
(60) Trolliard, G.; Benmechta, R.; Mercurio, D. *Acta Mater.* **2007**, *55*, 6011−6018.
(61) Zhou, J. K.; Zou, Z. G.; Ray, A. K.; Zhao, X. S. *Ind. Eng. Chem. Res.* **2007**, *46*, 745−749.
(62) Molla, A. R.; Tarafder, A.; Karmakar, B. *J. Mater. Sci.* **2011**, *46*, 2967−2976.
(63) Pei, L.; Li, M.; Liu, J.; Yu, B.; Wang, J.; Zhao, X. *Mater. Lett.* **2010**, *64*, 364−366.
(64) Aksel, E.; Jones, J. L. *J. Am. Ceram. Soc.* **2010**, *93*, 3012−3016.
(65) Navarro-Rojero, M. G.; Romero, J. J.; Rubio-Marcos, F.; Fernandez, J. F. *Ceram. Int.* **2010**, *36*, 1319−1325.
(66) Ribeiro, R. M.; Fiasca, A. B. A.; Santos, P. A. M.; Andreeta, M. R. B.; Hernandes, A. C. *Opt. Mater.* **1998**, *10*, 201−205.
(67) Hou, J. G.; Cao, R.; Jiao, S. Q.; Zhu, H. M.; Kumar, R. V. *Appl. Catal., B* **2011**, *104*, 399−406.
(68) Sakata, K.; Takenaka, T.; Naitou, Y. *Ferroelectrics* **1992**, *131*, 219−226.